Structural Engineering and Mechanics, *Vol. 68, No. 5 (2018) 549-561*
DOI: https://doi.org/10.12989/sem.2018.68.5.549

Global sensitivity analysis improvement of rotor-bearing system based on the Genetic Based Latine Hypercube Sampling (GBLHS) method

Mohammad Reza Fatehi[a], Afshin Ghanbarzadeh*, Shapour Moradi[b] and Ali Hajnayeb[c]

Mechanical Engineering Department, Shahid Chamran University of Ahvaz, Ahvaz 61355, Iran

(Received September 17, 2017, Revised January 23, 2018, Accepted October 23, 2018)

Abstract. Sobol method is applied as a powerful variance decomposition technique in the field of global sensitivity analysis (GSA). The paper is devoted to increase convergence speed of the extracted Sobol indices using a new proposed sampling technique called genetic based Latine hypercube sampling (GBLHS). This technique is indeed an improved version of restricted Latine hypercube sampling (LHS) and the optimization algorithm is inspired from genetic algorithm in a new approach. The new approach is based on the optimization of minimax value of LHS arrays using manipulation of array indices as chromosomes in genetic algorithm. The improved Sobol method is implemented to perform factor prioritization and fixing of an uncertain comprehensive high speed rotor-bearing system. The finite element method is employed for rotor-bearing modeling by considering Eshleman-Eubanks assumption and interaction of axial force on the rotor whirling behavior. The performance of the GBLHS technique are compared with the Monte Carlo Simulation (MCS), LHS and Optimized LHS (Minimax. criteria). Comparison of the GBLHS with other techniques demonstrates its capability for increasing convergence speed of the sensitivity indices and improving computational time of the GSA.

Keywords: global sensitivity analysis; sobol method; genetic based Latine hypercube sampling; rotor-bearing system; uncertainty analysis

1. Introduction

Nowadays, one of the main issues for scientists and engineers is to minimize uncertainty which is the behavior discrepancy between the model and real operation of the system. This minimization leads to increase reliability (Jafari *et al.* 2015, Liu *et al.* 2016, Muscolino *et al.* 2016) and fatigue life (Paolino *et al.* 2013), improved fault detection (Petryna *et al.* 2005), diagnosis and prognosis of systems (Mirzaee *et al.* 2015, Gobbato *et al.* 2012, Wei *et al.* 2015) and robust optimization (Guo *et al.* 2015, Zhao *et al.* 2014). The causes of the discrepancy are due to the aleatory uncertainty (e.g., parameter uncertainty, temporal and spatial variability known as natural variability) and epistemic uncertainty (e.g., model reduction or simplification known as modeling error). Inevitability of these causes makes uncertainty analysis crucial in the designing process of delicate systems.

Many studies have been conducted in the field of uncertainty analysis by statisticians and engineers (Paté-Cornell 1996, Faber 2005). From them, several studies have been conducted in the area of stochastic analysis of vibrating structures, which are summarized in Table 1. Uncertainty analysis. methods used in previous studies can be classified into two main categories: statistical techniques (e.g., crude Monte Carlo simulation in non-intrusive way and other sampling based methods) and non-statistical techniques (e.g., Neumann expansion method (Benaroya *et al.* 1988) and other stochastic finite element methods (Minh *et al.* 2016).

In the field of uncertainty analysis, from the real-life application viewpoint it is remarkable to determine which uncertainty sources are the most influential (factor prioritization strategy) and which of them are the least or non-influential (factor fixing strategy). The study of uncertainty influence (variation of input factors) on the output of a model can be accomplished by sensitivity analysis.

Rotor dynamic systems are among the important industrial cases which are exposed to a variety of uncertainty sources. Therefore, stochastic analysis of these systems is necessary, especially in high speed rotors. This study aimed to derive an efficient algorithm for sensitivity analysis (SA) of comprehensive rotordynamic systems to improve the computation time of the SA and sensitivity indices as an objective value.

In this paper, this objective is achieved by implementing an optimal form of stratified and non-overlapping sampling-based method (LHS), known as GBLHS. Development of this will be mainly focused in the SA phase and compared with classical methods (crude MCS). Among all of the sampling strategies, LHS is an orthogonal array sampling

*Corresponding author, Assistant Professor
E-mail: Ghanbarzadeh.A@scu.ac.ir
[a]Ph.D.
E-mail: mr-fatehi@phdstu.scu.ac.ir
[b]Professor
E-mail: moradis@scu.ac.ir
[c]Assistant Professor
E-mail: a.nayeb@scu.ac.ir

ISSN: 1225-4568 (Print), 1598-6217 (Online)

Table 1 Some outstanding studies in the field of Uncertainty Analysis (UA) of structural dynamic system

Contributor	Case Study and (uncertainty sources)	Methodology
Sinou *et al.* (2015) Didier *et al.* (2012a)	Rotor-shaft system	Polynomial chaos expansion (Iooss *et al.* 2000a) (PCE)
Didier *et al.* (2012b)	Nonlinear rotor system (misalignment, rotor bow, unbalance and rotor asymmetry)	Harmonic balance method and polynomial chaos expansion
Gan *et al.* (2015)	Jeffcott rotor with disc offset	Nonparametric modeling using random matrix theory (Saltelli *et al.* 2000a)
Ritto *et al.* (2011)	Robust optimization of a flexible rotor-bearing system (module of elasticity and shaft diameter)	Monte Carlo simulation
Stocki *et al.* (2012)	Rotor-shaft system (residual unbalances and bearing stiffness)	Optimal LHS
Szolc *et al.* (2009)	Rotor-shaft system (Crack detection)	Monte Carlo simulation
Liao *et al.* (2014)	Nonlinear rotor system (module of elasticity and asymmetric dimensions)	Harmonic balance method and polynomial chaos expansion
Sepahvand *et al.* (2013)	Orthotropic plate (Poisson's ratio and module of elasticity)	Extraction of Pdf of uncertain parameters using generalized PCE and inverse Pearson model
Kundu *et al.* (2014)	structural vibration of a corrugated panel (Elastic parameters)	Hybrid spectral and meta-modeling approach
Soize *et al.* (2000)	Vibration of linear structural dynamics	Nonparametric model of random uncertainties by random matrix theory
Duchereau *et al.* (2003)	Dural plates connected together considering random distributions of bolt prestresses	Constructing random uncertainties matrix model using nonparametric probabilistic method

method that ensures each subspace is evenly sampled. While MCS method are entirely random so that any given sample may fall anywhere within the range of the input distribution. This is the reason of excellence of LHS respect to MCS. However, LHS array can be optimized by different objectives that are given in next sections. In this paper, a novel strategy is presented to improve the LHS arrays using a new algorithm that maximize the minimum distance in a LHS array. The methodology is based on the genetic algorithm and the genetic operators are applied on the arrays indices with a new approach.

The Global Sensitivity Analysis (GSA) has been implemented which can overcomes the limitations of local methods (linearity, normality assumptions and local variations) (Iooss *et al.* 2015). It examines the whole variation in the input domain and the effect of one or several input factors (design variables) on the state variables or system outputs (Saltelli *et al.* 2000). As the Sobol's method is an efficient technique of GSA it will be used to obtain sensitivity indices. This method is a sampling based method with sampling strategy being an influential factor in the performance of the Sobol's method. In this paper the GBLHS strategy is presented and compared with other strategies such as: MCS, LHS, OLHS based in the minimax objective.

2. Sensitivity analysis

Factor fixing and factor prioritization as well as computing interactions and nonlinearity among factors are the most common strategies pursued in the field of GSA. A great deal has been done to develop different GSA fields and achieve higher computational efficiency, robustness and accuracy through different methodologies (Saltelli 2004, Saltelli 2008, Sobol 1993, Jourdan 2012). Among them, the most important methods are: 1) Local approach which is the derivative of output with respect to input factor. This method does not cover the whole variable domain (Saltelli *et al.* 2000). 2) Regression based approach which is a mapping between the input factors and system output. Then, metamodels regression is constructed and the output is expressed by a linear or nonlinear combination of input factors (Tondel *et al.* 2013, Lozzo *et al.* 2015). 3) Analysis of variance (ANOVA) which is based on the variance decomposition of the outputs (Krishnaiah 1981). Interaction between factors and nonlinearity effects of the metamodels can be exploited in this approach. 4) Screening approach which aims to analyze large dimensional models with a computationally cheap property. This approach is based on the computation of elementary effect and only the most important factors in a complex model are specified (Campolongo *et al.* 2007).

2.1 Qualitative SA base on the Morris method

Morris method is a prevalent screening approach which refer to as a one-factor-at-a-time (OAT) technique in the field of qualitative SA and applied in cases where there is a large number of inputs or heavy computation burden in the qualitative SA process. The method involves the ability to cope with the influence of scale and shape, multidimensional averaging, model independency and grouping factor analysis (Saltelli 2004). Two sensitivity measures are calculated in this method: The first is called mean (μ^*) which estimates the overall effect of a factor on the model output. The second is standard deviation (σ) which estimates interaction and nonlinearity of a factor with respect to other factors. This method has been presented in details by Saltelli *et al.* (Saltelli 2004, Saltelli 2008). In this method first the orientation matrix $\boldsymbol{T}$ which is a random sequence of N normalized samples $s_1, s_2, \dots, s_{N+1}$, is constructed. This matrix is a trajectory where these samples (s_i) have the following constraints: 1) Two consecutive sampling points have changed in one dimension only. 2) At least, every dimension has changed once in the trajectory. The randomized orientation matrix, $\boldsymbol{T}^*$, is given by (Morris 1991)

$$\boldsymbol{T}^* = \left(J_{N+1,1} G^* + \left(\frac{\Delta}{2} \right) \left[\left(2\mathrm{B} - J_{N+1,N} \right) D^* + J_{N+1,N} \right] \right) P^* \quad (1)$$

Where $J_{N+1,1}$ is an N+1-by-1 unit matrix, G^* represents a sample point from the set, B denotes an N+1-by-N matrix in which elements are 0s and 1s, and for every column, two rows of it are different only in the j_{th} entry (Saltelli 2004). D^* is an N-dimensional diagonal matrix made by either +1 or -1 with equal probability, Δ is step size in the trajectory, and finally P^* is an N-by-N random permutation matrix which is described in (Saltelli 2004). After extracting the randomized orientation matrix, input

Table 2 Several important researches in the field of OLHS

Contributor(s)	Methodology	Objective(s)
Morris and Mitchell (1995)	simulated annealing	Maximin and Maximize entropy
Jin *et al.* (2005)	enhanced stochastic evolutionary (ESE)	Intersite distance evaluation based on the new φ_p criteria
Grosso *et al.* (2009)	Iterated Local Search heuristics (ILS)	Maximin based on the φ_p criteria
Rennen *et al.* (2010)	Nested Latin hypercube designs	Maximin (space-filling nested design)
Ye *et al.* (2000)	A new columnwise-pairwise (CP) algorithm for searching optimal design within the SLHD	Maximize entropy and the minimum distance
Shields *et al.* (2016)	Latinized partially stratified sampling	Variance reduction

variables are generated. The sensitivity measures of input variables are evaluated by (Saltelli 2004)

$$\mu_i = \frac{\sum_{i=1}^{R} d_i}{R} \tag{2}$$

$$\sigma_i = \sqrt{\sum_{i=1}^{R} \left(d_i - \mu\right)^2 / R} \tag{3}$$

where R is the number of iterations, and d_i is the elementary effect of i_{th} input variable

$$d_i = \frac{\left[f\left(s(k+1)\right) - f\left(s\right) \right]}{\Delta} \tag{4}$$

2.2 Quantitative SA based on the Sobol method

Sobol method is an ANOVA based SA, which defines variance-based sensitivity indices in the context of high-dimensional integration (Sobol 1993). The method calculates sensitivity indices based on accurate calculation of the variance of the output, but it is more computationally prohibitive than Morris method. Sobol decomposition of the variance of the output Y is expressed as (Saltelli 2000b)

$$var\left(Y\right) = \sum_{i=1}^{k} D_i + \sum_{1 \le i \le j \le k} D_{ij} + \ldots + D_{1,2,\ldots,k} \tag{5}$$

Where

$$D_i = var\left(E\left(Y|x_i\right)\right) \tag{6}$$

$$D_{ij} = var\left(E\left(Y|x_i x_j\right)\right) - var\left(E\left(Y|x_i\right)\right) - var\left(E\left(\mathrm{Y}|x_j\right)\right) \tag{7}$$

It needs to note that the sensitivity indices are the input parameter contribution to the output variance, the fractional contribution of x_i to the variance of Y can be written as

$$S_i = \frac{D_i}{var\left(Y\right)} \tag{8}$$

S_{ij} measures the sensitivity of the interaction of the two input parameters $\mathrm{x_i}$ and $\mathrm{x_j}$ regardless of the effect of each parameter, individually

$$S_{ij} = \frac{D_{ij}}{var\left(Y\right)} \tag{9}$$

The total sensitivity index (ST_i) is defined as the sum of individual and interaction effect only for the input parameters, $\mathrm{x_i}$ (Saltelli *et al.* 2000b)

$$ST_i = S_{i1} + S_{i2} + \ldots + S_{ii} + \ldots + S_{iN} \tag{10}$$

Evaluation of D_i , D_{ij} ,… is commonly performed using an appropriate sampling method. In the next section, GBLHS technique will be introduced as an improved version of LHS method. Then, the accuracy and computational time of the Sobol method will be discussed and compared with Monte Carlo simulation (MCS) and LHS methods in the next section.

3. GBLHS strategy

A host of studies have been conducted evaluating of high dimensional metamodels and GSA. This can be performed by designing simulations in the sampling way such as: fractional factorial sampling, Monte Carlo simulation (MCS), quasi-random sampling (Quasi-MCS), LHS and etc. LHS is noteworthy because of its non-overlapping design among the mentioned sampling methods. LHS has been successfully used to generate multivariate samples of statistical distributions in the field of design of experiment (DOE). It was first proposed by McKay *et al.* (McKay *et al.* 1979). This method has been widely used in the field of computational stochastic mechanics (Olsson *et al.* 2002, Stocki *et al.* 2007), structural reliability (Olsson *et al.* 2003) and simulation of structural systems (black-box function evaluation). Various techniques have been presented to optimize the LHS method to achieve better space filling design (SFD). The orthogonality constraint of arrays should be considered in this method. Maximin distance in p-norm space (Johnson *et al.* 1990, Mitchell 1974), correlation (Vorechovsky *et al.* 2009), entropy and integrated mean squared-error (IMSE) criterion (Park 1994), and centered L_2 discrepancy (Hickernell 1998) are among the objective functions. Some of the most recent studies for generating of optimal LHS are presented in Table 2.

Under the variety of objectives, the optimal LHS can be achieved using evolutionary algorithms such as genetic algorithm (Crombecq *et al.* 2006), ESE (Jin *et al.* 2005) and simulated annealing (Morris *et al.* 1995). In this study, the generation of M optimal samples in N-dimensional space (N input factors) is accomplished based on the GBLHS algorithm. The details of the proposed algorithm is provided in a flowchart demonstrated in Fig 1. The genetic operators in each generation (mutation, crossover and elitism) are applied on the orthogonal sample arrays which are extracted by classical LHS method. The main contributions of this algorithm are given as follows:

1) After exploitation of the closest sample points in LHS array, their indices are extracted and then are introduced as chromosome in genetic algorithm. Considering this point, convergence speed of the minimax

value because of maintaining effective indices in the next generations, is increased significantly. This approach is one of the novelties of the proposed technique.

2) Crossover and mutation operations, which are performed with a novel strategy and are given in Sections 3.1 and 3.2, differing from other studies (e.g., (Jin *et al.* 2005)).

3) In this method, the objective function is the minimum distance of the sampling points in LHS array which has to be maximized.

4) There are some differences between the proposed algorithm and GA, in which the population size increases by crossover and mutation operations. It decreases to initial population size once the elitism and random generation (for avoiding local optimum stucking) are performed (Fig 1, step 13). Crossover, mutation and elitism processes are explained in sections 3.1 through 3.3.

5) The GBLHS algorithm that are depicted in Fig. 1 through 3, is elicited based on the performance examination of the different scenarios using tree-based genetic programing (GP) method. In tree-based GP, the mathematical expressions are represented in tree structures that are evaluated recursively to produce the resulting algorithm.

3.1 Crossover operation

In the GBLHS method, Crossover operation is applied to N_c number of the closest sample point pair in the LHS arrays in every iteration, where N_c is equal to floor function of $C_c N_p$

$$\mathbf{N}_c = \left[\mathbf{C}_c \mathbf{N}_p\right] \tag{11}$$

Where C_c is the crossover coefficient and $\mathbf{N}_p$ is the number of LHS arrays population. As indicated in Fig. 2, the distances between the projected closest sample point pairs in each dimension are computed and sorted. In the next step, the best R_c number of the dimensions is selected to apply crossover operation (Fig. 2). The main objective of this operation between sample pairs is to recombine worse indices which have minimum distances.

3.2 Mutation operation

Mutation is applied to $\mathbf{N}_m$ number of the closest sample point pair in the LHS arrays in every iteration, where $\mathbf{N}_m$ is equal to floor function of $\boldsymbol{C}_m \mathbf{N}_p$

$$\mathbf{N}_m = \left[\mathbf{C}_m \mathbf{N}_p\right] \tag{12}$$

Where $\boldsymbol{C}_c$ is the crossover coefficient. The mutation strategy is demonstrated in Fig 3. The J_{th} nearest sample pair (J=1: $\mathbf{N}_m$) will be mutated with two random selected samples from the LHS array. Comparison of the random index selection and proposed index selection (i.e., step 2 of crossover operation, Fig. 2) is demonstrated in Fig. 3.

3.3 Elitism operation

In every iteration, appropriate arrays with high objective values (i.e., maximum of minimum distance criteria) are maintained for the next iteration by applying elitism operation. The number of the best arrays is

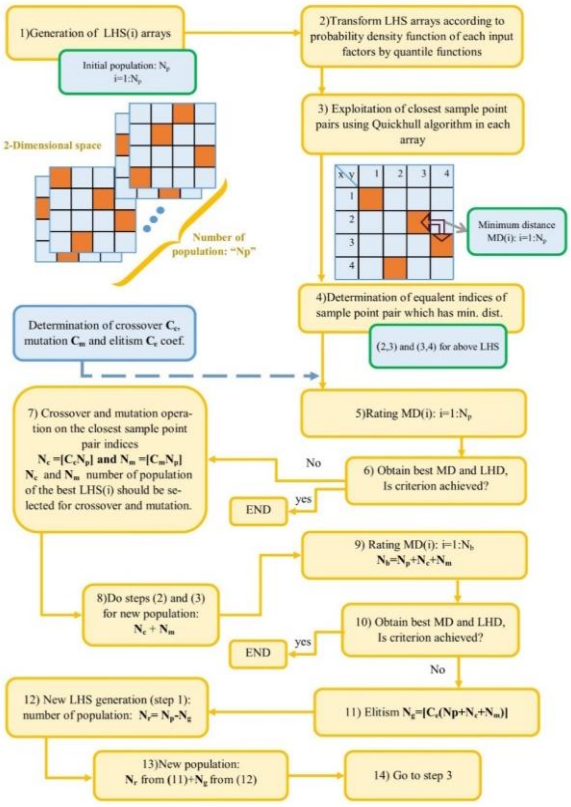

Fig. 1 GBLHS algorithm

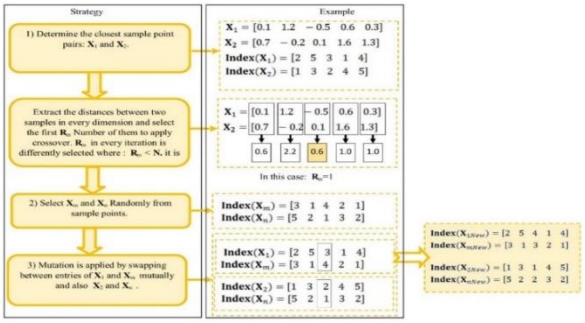

Fig. 3 Mutation operation

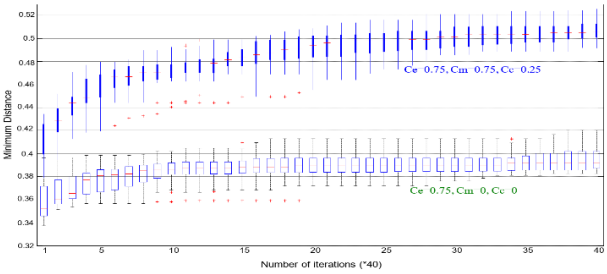

Fig. 4 Convergence of the best minimum distance using GBLHS method (Number of population: N_p=4, number of iterations=2000)-Effect of mutation and crossover operations to maximize objective (minimum distance)

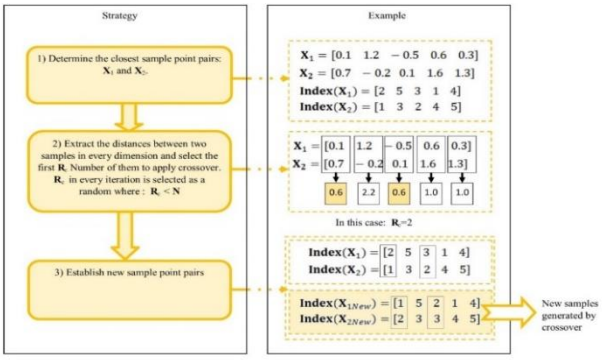

Fig. 2 Crossover operation

Table 3 Performance of the GBLHS method with different operator's coefficients

No. Test	No. pop.	C_e	C_c	C_m	Mean value computation time (sec.)	Expected value of the min. dist.
1	6	0.75	0.25	0.25	111	1.22
2	6	0.75	0.75	0.75	154	1.13
3	4	0.75	0.25	0.25	67	1.11
4	4	0.75	0.75	0.75	111	1.13
5	2	0.5	0.5	0.5	51	1.12

$$\mathbf{N}_g = [\mathbf{C}_e(\mathbf{N}_p + \mathbf{N}_c + \mathbf{N}_m)] \tag{13}$$

3.4 Convergence investigation

The effect of the operators applied in GBLHS method in comparison with the random search (considering elitism) is presented in Fig. 4, for an example in which the aim is to generate optimal LHS array with sample size 1000 (N) and four variables (M).

Each test is repeated 20 times with the results given in the boxplot form. Fig. 4 reveals that the GBLHS method ($\mathbf{C}_e = 0.75, \mathbf{C}_c = 0.25, \mathbf{C}_m = 0.75$) is superior to random search strategy ($\mathbf{C}_e = 0.75, \mathbf{C}_c = 0, \mathbf{C}_m = 0$) and the minimum distance is converged with a high convergence rate.

The performance of the proposed method was investigated by examining the effects of the operator's coefficient values to generate OLHS arrays with $N = 300$ *and* $M = 20$ (Table 3). Every test was repeated 10 times and the number of iterations is equal to 500. The results indicated that the crossover coefficient greater than 0.5 is not an efficient value for the algorithm and increasing initial population has major effect on the computation time while a minor effect on the objective value.

3.5 Efficiency evaluation by high dimensional function computation

The performance of the proposed method (GBLHS) was compared with LHS and Monte-Carlo simulation methods through evaluating high-dimensional function and sensitivity analysis considering the interaction between the parameters (input factors). Initially, evaluation of the Rosenbrock function will be estimated, which is expressed as

Table 4 Estimation of Rosenbrock function using different sampling methods

Method	Standard deviation of the evaluations (Rosen rock function), Mean Value=175.5
Monte Carlo simulation	3.51
LHS	3.07
OLHS (maximin, random search, 1200 iterations)- using MATLAB Software R2013b.	3.01
GBLHS (min.dist., 400 iterations)	2.84

$$f(x) = \sum_{i=1}^{n-1}(100(x_{i+1} - x_i^2)^2 + (x_i - 1)^2) \tag{14}$$

With generation of each array (300×10 dimensions), the mean value of fitness of the test functions was evaluated by 300 samples in a high-dimensional case (n=10) in every practice, with each input factor being generated from uniform distribution as $x_i \in U(0,1)$. Performance of each method was estimated by evaluating the standard deviation of mean values of 180 practices. Lower values of standard deviation demonstrated better estimation of the test function. GBLHS has given low standard deviation compared to other methods (Table 4). The performance of the Rosenbrock function improved by about 7.5% and 5.9% compared to LHS and OLHS (Proposed algorithm in MATLAB Software: lhsdesign command) respectively.

Performance of the GBLHS method in the SA using Sobol method compared with other techniques with the results tabulated in Table 5. A 10-dimensional function is given as

$$f = x_1^2 + x_2^2 + x_3 + x_4 + x_1^2 x_5 + x_6 + x_7 + x_8^2 + x_9 + x_{10} \tag{15}$$

Where $x_i \in \boldsymbol{U}(0,3)$. The SA indices of different techniques are shown in Fig 5. It is clear that parameters x_1, x_2, x_5 and x_8 are more effective than the other parameters because of their higher degrees of polynomial (x_1, x_2, x_8) and the interactive effects between x_1 and x_5.

Here, the relative error is introduced as a criterion to estimate the performance of each technique. It express the difference of the sensitivity indices with respect to MCS considering 4,000,000 simulations. The relative error parameter is defined as

$$E = \frac{\sum_{i=1}^{M} |S_{i\,MCS} - S_i|}{\sum_{i=1}^{M} S_{i\,MCS}} \tag{16}$$

Where $S_{i\,MCS}$ is the extracted sensitivity index of i_{th} factor using MCS and S_i is the sensitivity index of i_{th} factor using intended method. According to relative error

Table 5 Relative error in estimation of sensitivity indices using MCS, OLHS and GBLHS

Method and control parameters	No. of the simulations	Relative error
Monte Carlo simulation (reference case)	4,000,000	-
OLHS (Minimax,2000 iterations)	2,000	0.12
GBLHS (10 iterations)	2,000	2.48
GBLHS (100 iterations)	2,000	0.46
GBLHS (2000 iterations)	2,000	0.03

Table 6 Computational time of different sampling techniques to achieve relative error (E=0.02)

Sampling technique	Computational time (sec.)
Monte Carlo simulation (reference case)	-
LHS	184.1
OLHS (Minimax Citeria)	59.1
OLHS (ESE)	56.1
GBLHS	54.4

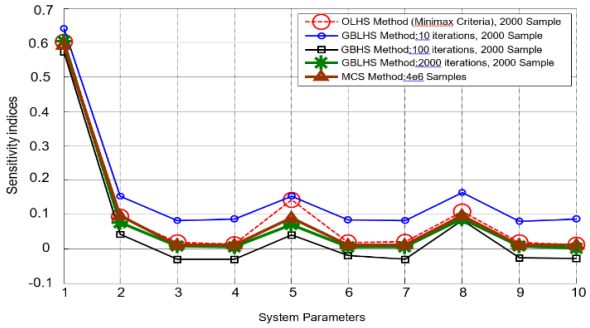

Fig. 5 Comparing different sampling methods to estimate SA indices

values presented in Table 5 and the results presented in Fig 5, the closest result to the reference mode (MCS with 4.0e6 simulations) has been achieved using GBLHS method with 2000 simulations and 2000 iterations.

Efficiency of the GBLHS algorithm is investigated by computational time. Taking into considering equal relative error as an objective ($E = 0.02$) in estimation of sensitivity indices of the multidimensional function f, computational time of different methods are given in Table 6 for 25 experiments. The results show that the GBLHS technique as an optimal stratified and non-overlapping samples is faster than OLHS (Minimax criteria, ESE), for the reason that the convergence criteria is achieved by fewer samples than other techniques.

4. Rotordynamic modeling

Rotordynamic systems are among the important industrial cases which are exposed to a variety of uncertainty sources, hence stochastic analysis of these systems is necessary, especially in high speed rotors. In this

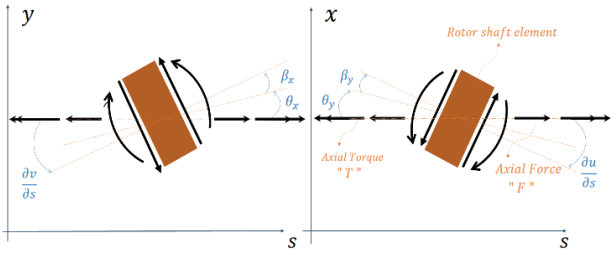

Fig. 6 Rotor element considering interaction of torque and axial force

paper, many uncertain physical and dimensional factors are considered by introducing of Eshleman-Eubanks assumption. Improved GSA by GBLHS algorithm is applied on the rotor-bearing system to omit non-influential factors. The partial differential equation of motion of the rotor system was extracted using a continuous model, while taking into account the effect of the gyroscopic moment, rotary inertia, and shear deformation.

To have a more reliable analysis in this model, the interaction of the axial torque (T) (Eshleman-Eubank assumption) and axial force (F) on whirling behavior of the rotor was considered, simultaneously. The force and momentum components of rotor-shaft element are indicated in Fig. 6 with u and v representing the whirling amplitudes of the rotor and θ_i and β_i denoting bending and shear angles, respectively. Therefore, the governing differential equations of motion for the rotor can be described by the following relations

$$\begin{Bmatrix} EI\frac{\partial^2\theta_y}{\partial s^2}+T\frac{\partial\theta_x}{\partial s}+\mathrm{K}AG\frac{\partial u}{\partial s}-\mathrm{K}AG\theta_y-F\theta_y=\rho I\left(\frac{\partial^2\theta_y}{\partial t^2}-2\frac{\partial\theta_x}{\partial t}\omega\right) \\ EI\frac{\partial^2\theta_x}{\partial s^2}-T\frac{\partial\theta_y}{\partial s}+\mathrm{K}AG\frac{\partial v}{\partial s}-\mathrm{K}AG\theta_x-F\theta_x=\rho I\left(\frac{\partial^2\theta_x}{\partial t^2}+2\frac{\partial\theta_y}{\partial t}\omega\right) \\ \mathrm{K}AG\frac{\partial^2 u}{\partial s^2}-\mathrm{K}AG\frac{\partial\theta_y}{\partial s}=\rho A\frac{\partial^2 u}{\partial t^2} \\ \mathrm{K}AG\frac{\partial^2 v}{\partial s^2}-\mathrm{K}AG\frac{\partial\theta_x}{\partial s}=\rho A\frac{\partial^2 v}{\partial t^2} \end{Bmatrix} \quad (17)$$

Using the weighted residual method, the residual terms ($\mathcal{R}_i$) can be extracted from the continuous partial differential equations as

$$\begin{Bmatrix} \mathrm{R}_1=\rho I\left(\frac{\partial^2\tilde{\theta}_y}{\partial t^2}-2\frac{\partial\tilde{\theta}_x}{\partial t}\omega\right)-EI\frac{\partial^2\tilde{\theta}_y}{\partial s^2}-T\frac{\partial\tilde{\theta}_x}{\partial s}-\mathrm{K}AG\frac{\partial\tilde{\mathbf{u}}}{\partial s}+\mathrm{K}AG\tilde{\theta}_y+F\tilde{\theta}_y \\ \mathrm{R}_2=\rho I\left(\frac{\partial^2\tilde{\theta}_x}{\partial t^2}+2\frac{\partial\tilde{\theta}_y}{\partial t}\omega\right)-EI\frac{\partial^2\tilde{\theta}_x}{\partial s^2}+T\frac{\partial\tilde{\theta}_y}{\partial s}-\mathrm{K}AG\frac{\partial\tilde{\mathbf{v}}}{\partial s}+\mathrm{K}AG\tilde{\theta}_x+F\tilde{\theta}_x \\ \mathrm{R}_3=\rho A\frac{\partial^2\tilde{\mathbf{u}}}{\partial t^2}-\mathrm{K}AG\frac{\partial^2\tilde{\mathbf{u}}}{\partial s^2}+\mathrm{K}AG\frac{\partial\tilde{\theta}_y}{\partial s} \\ \mathrm{R}_4=\rho A\frac{\partial^2\tilde{\mathbf{v}}}{\partial t^2}-\mathrm{K}AG\frac{\partial^2\tilde{\mathbf{v}}}{\partial s^2}+\mathrm{K}AG\frac{\partial\tilde{\theta}_x}{\partial s} \end{Bmatrix} \quad (18)$$

Where $\tilde{\mathbf{Q}}=\langle\tilde{\mathbf{u}},\ \tilde{\mathbf{v}},\ \tilde{\boldsymbol{\theta}}_x,\tilde{\boldsymbol{\theta}}_y\rangle$ is the approximate solution of the $\mathbf{Q}=\langle\mathbf{u},\ \mathbf{v},\ \boldsymbol{\theta}_x,\ \boldsymbol{\theta}_y\rangle$ which is calculated according to the following equations

$$\tilde{\mathbf{Q}}=\begin{bmatrix} N_x \\ N_y \\ M_x \\ M_y \end{bmatrix}.\mathfrak{Q}=\mathrm{S}\,\mathfrak{Q} \quad (19)$$

The relation $\sum R_i = 0$ is used to extract weak form of the equation of motion.

$$\begin{cases} \mathbf{R}_1 = \int_0^l \{M_y\} \mathrm{R}_1 = 0 \\ \mathbf{R}_2 = \int_0^l \{M_x\} \mathrm{R}_2 = 0 \\ \mathbf{R}_3 = \int_0^l \{N_y\} \mathrm{R}_3 = 0 \\ \mathbf{R}_4 = \int_0^l \{M_x\} \mathrm{R}_4 = 0 \end{cases} \tag{20}$$

The shape functions, $\mathcal{S}$, are given in Appendix A. The weak form of Eq. (17) based on the weighted residual method and Bubnov-Galerkin approach are given as

$$\boldsymbol{M}_{eq} = \int_0^l [\rho I(\{M_y\}^T \{M_y\} + \{M_x\}^T \{M_x\}) + \rho A\left(\{N_y\}^T \{N_y\} + \{N_x\}^T \{N_x\}\right)]ds \tag{21}$$

$$\boldsymbol{K}_{eq} = K_{el} + K_f + K_T \tag{22}$$

$$\boldsymbol{C}_{eq} = \int_0^l [2\rho I\omega(\{M_y\}^T \{M_x\} - \{M_x\}^T \{M_y\})]ds \tag{23}$$

$$\boldsymbol{K}_f = \int_0^l [F(\{N_y^{'}\}^T \{N_y^{'}\} + \{N_x^{'}\}^T \{N_x^{'}\})]ds \tag{24}$$

$$\boldsymbol{K}_T = \int_0^l [T(\{M_y\}^T \{W_x^{'}\} + \{M_x\}^T \{M_y^{'}\})]ds \tag{25}$$

$$\boldsymbol{K}_{EI} = \int_0^l [EI(\{M_y^{'}\}^T \{M_y^{'}\} + \{W_x^{'}\}^T \{W_x^{'}\})]ds \tag{26}$$

$$K_{el} = K_{EI} + K_{sh} \tag{27}$$

The above matrices are calculated and given in Appendix B. The details of the calculated matrices above are given in Appendix B. Using the above weak forms and the relation, the general equation of rotor motion can be expressed as

$$\boldsymbol{M}_{eq} \ddot{\tilde{\mathbf{Q}}} + \boldsymbol{C}_{eq} \dot{\tilde{\mathbf{Q}}} + \boldsymbol{K}_{eq} \tilde{\mathbf{Q}} = \boldsymbol{F} \tag{28}$$

Where $\mathrm{M_{eq}}$, $\boldsymbol{C}_{eq}$ and K_{eq} are the equivalent mass, damping and stiffness, respectively. The rotor systems are under the influences of several uncertainty sources such as structural damping, stiffness and damping of the supports, centrifugal forces, blade mistuning, density and module of elasticity of the material etc. Investigating the effect of the uncertain parameters of a rotor-bearing system will be done by two SA method through a case study.

4.1 Rotor-bearing case study

The SA of rotordynamic system was performed at different speeds with the objective of studying the whirling frequencies of the rotor in different modes. Axial torque and force, module of elasticity, density, Poisson's ratio, rolling element bearing (REB) stiffness and rotor shaft and disc dimensions were the uncertain parameters whose effects were investigated using SA strategies. Since the probability density function (PDF) of the uncertain parameters is essential to obtain validated results, it would be implemented in the algorithm using Sobol method. Initially, using Morris method, which is a screening based technique, the minor influential parameters were omitted and defined as deterministic parameters.

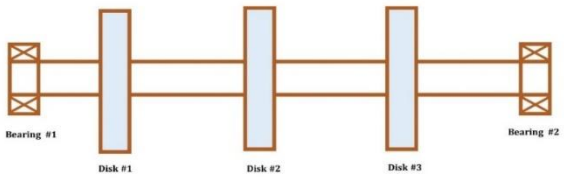

Fig. 7 Rotor-bearing case study

Table 7 Uncertain parameters in rotor-bearing case study

Element name	Properties	
Rotor shaft	Diameter	$U(30,30.5)$ (mm)
	Length (L)	$U(680,684)$ (mm)
	Density ρ	$U(7700,7854)$ (kg/m^3)
	Poisson's ratio ϑ	$U(0.30,0.33)$
	Module of elasticity E (with the consideration of random field)	$U(1.9e11,1.938e11)$ Gpa
Excitations	Torque (T)	$U(0,2000)$ (N.m)
	Axial force (F)	$U(0,2000)$ (N)
Disk #1 Station: 10 cm	Radius (rd1)	$U(100,101)$ (mm)
	Mass (md1)	$U(1,1.01)$ (kg)
Disk #2 Station: 30 cm	Radius (rd2)	$U(100,101)$ (mm)
	Mass (md2)	$U(1,1.01)$ (kg)
Disk #3 Station: 50 cm	Radius (rd3)	$U(100,101)$ (mm)
	Mass (md3)	$U(1,1.01)$ (kg)
Bearings #1 and #2 Station: two ends of the rotor shaft	Stiffness	$K_{xx} = U(1.5e8,3e8)$ (N/m) $K_{yy} = U(1.5e8,3e8)$ (N/m) $K_{\theta x \theta x} = U(1500,2250)$ (N/m) $K_{\theta y \theta y} = U(1500,2250)$ (N/m)

Next, the major influential parameters were analyzed precisely using Sobol method to compute sensitivity indices considering PDF of the parameters. The uncertain parameters were then applied to the case study as shown in Fig. 7, with the parameter value with their PDF's given in Table 7.

4.2 Initial SA using Morris method

All the proposed uncertain parameters in Table 7 are considered to be analyzed using Morris method. Although this method gives qualitative and approximate results, it can be applied to decide on removing the minor effect parameters. The domain of the parameter variation in the case of SA using Morris method is given in Table 7. Determination of the exact value of the REB stiffness matrix is a challenging issue. Lately, Gou and Parker (Guo *et al.* 2012) introduced a FEM based methodology to extract

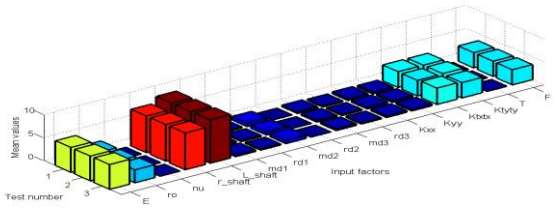

Fig. 8 Mean value of Morris SA indices, mode 1 backward whirling, rotor spining: 1000 rad/s

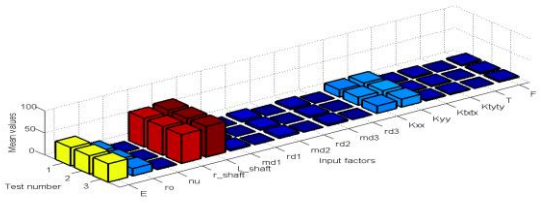

Fig. 9 Mean value of Morris SA indices, mode 3 forward whirling, rotor spining: 1000 rad/s

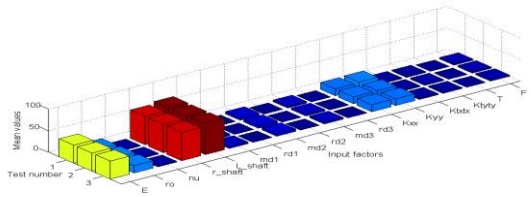

Fig. 10 Mean value of Morris SA indices, mode 3 forward whirling, rotor spining: 5000 rad/s

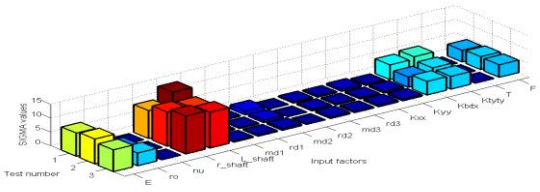

Fig. 11 Sigma value (σ) of Morris SA indices, mode 1 backward whirling, rotor spinning: 1000 rad/s

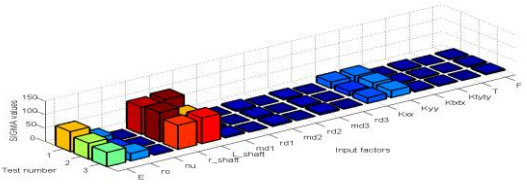

Fig. 12 Sigma value of Morris SA indices, mode 3 forward whirling, rotor spining: 1000 rad/s

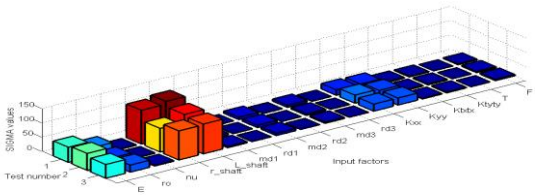

Fig. 13 Sigma value of Morris SA indices, mode 3 forward whirling, rotor spinning: 5000 rad/s

the stiffness matrix of a REB and compared it with other methods (e.g., COBRA (Jones *et al.* 1966) and REBM (Lim *et al.* 1990)). Since the modeling errors are the main source of uncertainty in the stiffness matrix evaluation, the range of the variability of stiffness values depends on the proposed strategies, where in this study the values employed in (Guo *at al.* 2012) have been implemented. Determinatio of the uncertainty range of the material properties and geometrical dimensions is based on the probable machining and assembling errors. Since the axial torque and forces are proportional to the loading conditions, their values vary within a wide range. The SA results are provided in Figs. 8 through 13. For extracting more reliable results, Morris test was repeated three times, at each rotor speed. It is obvious which of the parameters has a minor or major effect on the first (backward) and third (forward) whirling frequencies at different rotor speeds. It is concluded that at the rotation speed of 1000 rad/s, module of elasticity, density, rotor shaft radius and length, disc mass, bearing stiffness coefficients and axial force are the most important parameters in the mean and sigma values. As demonstrated in Fig 8 and 9, the effect of stiffness variations in the first mode is lower than in the third mode. Further, the parameter variations in the third rotor mode at different rotor speeds (1000 rad/s and 5000 rad/s) give similar effects, according to Figs. 9 and 10. At the rotation speed of 5000 rad/s, the effect of the mass and radius of the discs are greater than that of rotational speed 1000 rad/s (because of the gyroscopic effect). However, it is not significant when compared to the other effective parameters. The mean and sigma values have the same results in every modes and rotor speeds, qualitatively (e.g. compare Figs. 8 and 11). The results of the case study revealed that the effect of the axial force on the whirling frequency of the rotor is influential only in the first whirling mode and the axial torque is non-influential across of the modes with different rotor speeds.

It should be noted that the domain of the variation in parameters depends on the uniform distribution function given in Table 7. Next, a variance-based method namely Sobol method, which uses an optimized sampling method (GBLHS), was used to extract the measurable quantity of SA indices of rotor-bearing problem.

4.3 SA using Sobol method

Although the computational time of the variance-based algorithms is long, they are more accurate than the screening methods. Previously, 8 of the 17 parameters were omitted from the list of the uncertain parameters using Morris method. The remaining 9 parameters were analyzed with the PDF of each parameter given in Table 8. After generating a 2000×9 matrix using GBLHS, SA was

Table 8 Uncertain parameters with different PDF that are used in Sobol's method

Element name	Properties	
Rotor shaft	Rotor shaft diameter	$N(30.25,0.01)$ (mm)
	Rotor length (L)	$N(682,1)$ (mm)
	Density ρ	G (7770,900) (kg/m^3)
	Module of elasticity E (with the consideration of random field)	$N(1.920e11,4e18)$ (Gpa)
Excitations	Axial force (F)	$U(0,2000)$ (N)
Bearings #1 and #2 Station: two ends of the rotor shaft	Stiffness	$K_{xx} = U(1.5e8,3e8)$ (N/m) $K_{yy} = U(1.5e8,3e8)$ (N/m) $K_{\theta x\theta x} = U(1500,2250)$ (N/m) $K_{\theta y\theta y} = U(1500,2250)$ (N/m)

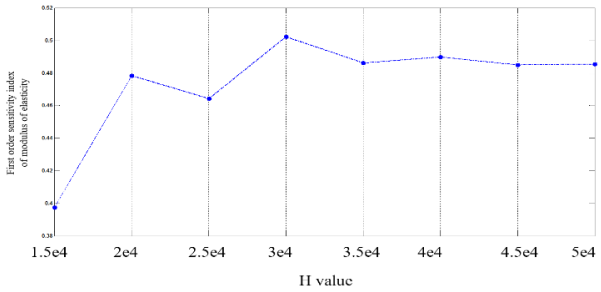

Fig. 14 Convergence of the first order sensitivity index of the module of elasticity by increasing sampling size and number of iteration

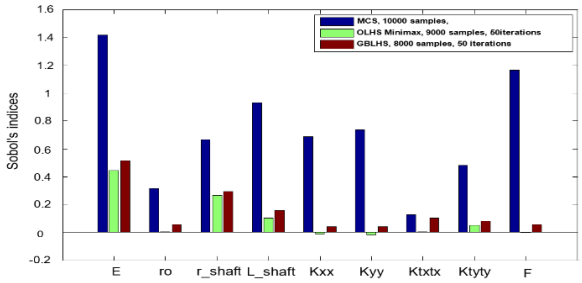

Fig. 15 Comparison of SA indices using MCS, OLHS (Minmax) and GBLHS methods, sensitivity of the first backward whirling frequency in rotor speed of 1000 rad/s

performed on the rotor-bearing FEM-based model.

The rotor shaft diameter, rotor length and module of elasticity were all assumed to have normal distributions. The density had gamma distribution and the axial force and bearing stiffness had uniform distribution functions. Convergence of the sensitivity indices of the module of elasticity with increase in the number of samples is demonstrated in Fig. 14. The results revealed that by increasing the number of population and iterations (i.e., the H value which is the number of population multiplied by the number of iterations), the sensitivity indices converge to a constant value. Moreover, the SA indices using MCS, OLHS and GBLHS methods are illustrated in Fig. 15. As can be seen from the figure, sampling strategy based on the GBLHS method has faster convergence than OLHS (i.e., minimax criteria) and MCS. The results showed that GBLHS using fewer sampling data, gives better

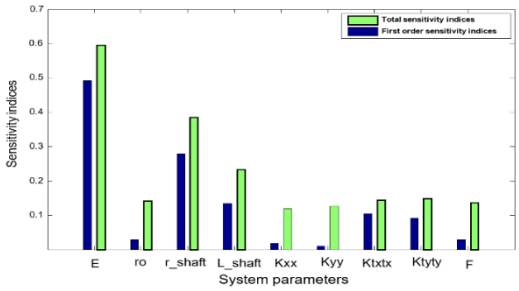

Fig. 16 SA indices values (Total and first order) using GBLHS (12000 samples and 100 iterations) in the first mode backward whirling at rotor rotation speed 1000 rad/s

convergence in comparison with other methods. First-order sensitivity indices are given in Fig 15.

One outstanding aspect of this case study is that while it considers different types of PDF in the input factors (i.e., normal, uniform and gamma distribution functions), it will converge faster if all input factors have the same PDF. The total and first order sensitivity indices for 12000 samples (100 iterations) are presented in Fig. 16.

Modulus of elasticity, shaft radius, shaft length and bearing stiffness are the most sensitive parameters in the proposed domains on whirling speed of the rotor-bearing system. Evidently, altering the PDF of input factors and their parameters will change the sensitivity indices.

5. Conclusions

Sensitivity analysis was performed on a high speed rotor-bearing system to accomplish uncertainty analysis considering different types of input factor PDF's. The sampling strategy was developed by GBLHS method as a new method. The Eshleman-Eubanks assumption and axial force interaction effect were implemented in rotor shaft elements to attain more reliable result and decrease modeling errors. As a case study, the Morris method was implemented on 20 uncertain parameters to pretermit insensitive parameters which resulted in nine sensitive parameters. Use of GBLHS method as an accurate and efficient sampling strategy in the Sobol sensitivity analysis improves the results of the SA by decreasing sampling size needed to estimate SA indices. The relative error of the GBLHS method in SA of a multi-dimensional function was clearly less than that of other mentioned techniques (e.g. LHS, OLHS the Matlab toolbox 'lhsdesign'). The performance of the GBLHS method was investigated by sensitivity analysis of the rotor-bearing system. The results indicated the effectiveness of the GBLHS method compared to the MCS, OLHS, etc. Finally, convergence conditions and performance of the proposed method were investigated and compared with MCS and OLHS (Minimax criteria) methods.

References

Benaroya, H. and Rehak, M. (1988), "Finite element methods in

probabilistic structural analysis: A selective review", *Appl. Mech. Rev.*, **41**(5), 201-213.
Campolongo, F., Carboni, J. and Saltelli, A, (2007), "An effective screening design for sensitivity analysis of large models", *Environ. Modell. Softw.*, **22**, 1509-1518.
Crombecq, K. and Dhaene, T. (2006), "Generating sequential space-silling designs using genetic algorithms and Monte Carlo methods", *Comput. Indust. Eng.*, **50**, 503-527.
De Lozzo, M. and Marrel, A. (2015), "Estimation of the derivative-based global sensitivity measures using a Gaussian process metamodel", *SIAM/ASA J. Uncertain. Quantific.*, **4**, 708-738.
Didier, J., Faverjon, B. and Sinou, J.J. (2012), "Analyzing the dynamic response of a rotor system under uncertain parameters by polynomial chaos expansion", *J. Vibr. Contr.*, **18**, 587-607.
Didier, J., Sinou, J.J. and Faverjon, B. (2012), "Study of the nonlinear dynamic response of a rotor system with faults and uncertainties", *J. Sound Vibr.*, **331**, 671-703.
Duchereau, J. and Soize, C. (2003), "Transient dynamic induced by shocks in stochastic structures", *Appl. Stat. Probab. Civil ICASP*, **9**, 1-6.
Faber, M.H. (2005), "On the treatment of uncertainties and probabilities in engineering decision analysis", *J. Offshore Mech. Arct. Eng.*, **127**, 243-248.
Gan, C., Wang, Y., Yang, S. and Cao, Y. (2014), "Nonparametric modeling and vibration analysis of uncertain Jeffcott rotor with disc offset", *Int. J. Mech. Sci.*, **76**, 126-134.
Gobbato, M., Conte, J., Koshmatka, J. and Farra, C. (2012), "A reliability-based framework of fatigue damage prognosis of composite aircraft structures", *Probab. Eng. Mech.*, **29**(1), 176-188.
Grosso, A., Jamali, A.R.M.J.U. and Locatelli, M. (2009), "Finding maximin Latin hypercube designs by iterated local search heuristics", *Eurz. Oper. Res. J.*, **197**(2), 541-547.
Guo, X., Zhao, X., Zhang, W., Yan, J. and Sun, G. (2015), "Multi-scale robust design and optimization considering load uncertainties", *Comput. Meth. Appl. Mech. Eng.*, **283**, 994-1009.
Guo, Y. and Parker, R.G. (2012), "Stiffness matrix calculation of rolling element bearings using a finite element/contact mechanics model", *Mech. Mach. Theor.*, **51**, 32-45.
Hickernell, F.J. (1998), "A generalized discrepancy and quadrature error bound", *Math. Comput.*, **67**, 299-322.
Iooss, B. and Lemaître, P. (2015), *A Review on Global Sensitivity Analysis Methods*, Meloni, C. and Dellino, *G. Uncertainty Management in Simulation-Optimization of Complex Systems: Algorithms and Applications*, Springer.
Jafari, P. and Jahani, E. (2016), "Reliability sensitivities with fuzzy random uncertainties using genetic algorithm", *Struct. Eng. Mech.*, **60**(3), 413-431.
Jin, R., Chen, W. and Sudjianto, A. (2005), "An efficient algorithm for constructing optimal design of computer experiments", *J. Stat. Plan. Infer.*, **51**, 268-287.
Johnson, M.E., Moore, L.M. and Ylvisaker, D. (1990), "Minimax and Maximin distance design", *J. Stat. Plan. Infer.*, **24**, 131-148.
Jones, A.B. and Poplawski, J. (1966), "A computer study of design parameters on rolling element bearing performance", *Proceedings of the Bearings Conference at Dartmouth University*.
Jourdan, A. (2012), "Global sensitivity analysis using complex linear models", **22**, 823-831.
Krishnaiah, P.R. (1981), *Analysis of Variance*, Elsevier, New York, U.S.A.
Kundu, A., DiazDelaO, F.A., Adhikari, S. and Friswell, M.I. (2014), "A hybrid spectral and metamodeling approach for the stochastic finite element analysis of structural dynamic systems", *Comput. Meth. Appl. Mech. Eng.*, **270**, 201-219.
Liao, H. (2014), "Global resonance optimization analysis of nonlinear mechanical systems: Application to the uncertainty quantification problems in rotor dynamics", *Commun. Nonlin. Sci. Numer. Simulat.*, **19**(9), 3323-3345.
Lim, T.C. and Singh, R. (1990), "Vibration transmission through rolling element bearings, part I: Bearing stiffness formulation", *J. Sound Vibr.*, **139**, 179-199.
Liu, Y., Jeong, H.K. and Collette, M. (2016), "Efficient optimization of reliability-constrained structural design problems including interval uncertainty", *Comput. Struct.*, **277**, 1-11.
McKay, M.D., Conover, W.J. and Beckman, R.J. (1979), "A comparison of three methods for selecting values of input variables in the analysis of output from a computer code", *Technometr.*, **21**(2), 239-245.
Michael, D., Shields, N. and Zhang, J. (2016), "The generalization of Latin hypercube sampling", *Reliab. Eng. Syst. Safety*, **148**, 96-108.
Minh, D.D., Gao, W. and Song, C. (2016), "Stochastic finite element analysis of structures in the presence of multiple imprecise random field parameters", *Comput. Meth. Appl. Mech. Eng.*, **300**, 657-688.
Mirzaee, A., Shayanfar, M. and Abbasnia, R. (2015), "A novel sensitivity method to structural damage estimation in bridges with moving mass", *Struct. Eng. Mech.*, **54**(6), 1217-1244.
Mitchell, T.J. (1974), "Computer construction of d-optimal first-order designs", *Technometr.*, **16**, 211-220.
Morris, M.D. (1991), "Factorial sampling plans for preliminary computational experiments", *Technometr.*, **33**, 161-174.
Morris, M.D. and Mitchell, T.J. (1995), "Exploratory designs for computer experiments", *J. Stat. Plan. Infer.*, **43**, 381-402.
Muscolino, G., Santoro, R. and Sofi, A. (2016), "Reliability assessment of structural systems with interval uncertainties under spectrum-compatible seismic excitation", *Probab. Eng. Mech.*, **44**, 138-149.
Olsson, A.M.J. and Sandberg, G.E. (2002), "On Latin hypercube sampling for stochastic finite element analysis", *J. Eng. Mech.*, **128**(1), 121-125.
Olsson, G., Sandberg, O. and Dahlblom. (2003), "On Latin hypercube sampling for structural reliability analysis structural safety", **25**, 47-68.
Paolino, D.S., Chiandussi, G. and Belingardi, G. (2013), "Uncertainty in fatigue loading: Consequences on statistical evaluation of reliability in service", *Probab. Eng. Mech.*, **33**, 38-46.
Park, J. (1994), "Optimal Latin-hypercube designs for computer experiments", *J. Stat. Plan. Infer.*, **39**, 95-111.
Paté-Cornell, M.E. (1996), "Uncertainties in risk analysis: Six levels of treatment", *Reliab. Eng. Syst. Safety*, **54**, 95-111.
Petryna, Y.S. and Kratzig, W.B. (2005), "Compliance-based structural damage measure and its sensitivity to uncertainties", *Comput. Struct.*, **83**, 1113-1133.
Rafał, S., Piotr, T. and Michał, K. (2007), "Efficient sampling techniques for stochastic simulation of structural systems", *Comput. Assist. Mech. Eng. Sci.*, **14**, 127-140.
Rennen, G., Husslage, B., Van Dam, E.R. and Hertog, D. (2010), "Nested maximin Latin hypercube designs", *Struct. Multidisc. Optim.*, **41**, 371-395.
Ritto, T.G., Lopez, R.H., Sampaio, R. and Souza, J.E. (2011), "Robust optimization of a flexible rotor-bearing system using the Campbell diagram", *Eng. Optim.*, **43**, 77-96.
Saltelli, A., Chan, K. and Scott, E.M. (2000a), *Sensitivity Analysis*, Wiley Series in Probability and Statistics, Wiley.
Saltelli, A., Ratto, M., Andres, T., Cariboni, J., Gatelli, D., Tarantola, S., Campolongo, F. and Saisana, M. (2008), *Global Sensitivity Analysis*, The Primer, John Wiley & Sons, U.S.A.
Saltelli, A., Tarantola, S. and Campolongo, F. (2000b),

"Sensitivity analysis as an ingredient of modeling", *Stat. Sci.*, **15**, 379-390.
Saltelli, A., Tarantola, S., Campolongo, F. and Ratto, M. (2004), *Sensitivity Analysis in Practice, A guide to Assesing Scientific Models*, John Wiley & Sons, U.S.A.
Sepahvand, K. and Marburg, S. (2013), "On construction of uncertain material parameters using generalized polynomial chaos expansion from experimental data", *Proc. IUTAMG.*, 4-17.
Sinou, J.J. and Jacqueliin, E. (2015), "Influence of polynomial chaos expansion order on an uncertain asymmetric rotor system response", *Mech. Syst. Sign. Proc.*, **50**, 718-731.
Sobol, I.M. (1993), "Sensitivity analysis for non-linear mathematical models", *Math. Model. Comput. Exper.*, **1**, 407-414.
Sobol, I.M. (1993), "Sensitivity analysis for non-linear mathematical models", *Math. Model. Comput. Exper.*, **1**, 407-410.
Soize, C. (2000), "A nonparametric model of random uncertainties for reduced matrix models in structural dynamics", *Probab. Eng. Mech.*, **15**, 277-294.
Stocki, R., Szolc, T., Tauzowski, P. and Knabel, J. (2012), "Robust design optimization of the vibrating rotor-shaft system subject to selected dynamic constraints", *Mech. Syst. Sign. Proc.*, **29**, 34-44.
Szolc, T., Tauzowski, P., Stocki, R. and Knabl, J. (2009), "Damage Identification in vibrating rotor-shaft systems by efficient sampling approach", *Mech. Syst. Sign. Proc.*, **23**, 1615-1633.
Tondel, K., Vik, J.O., Martens, H., Indahl, U.G., Smith, N. and Omholt, S.W. (2013), "Hierarchical multivariate regression-based sensitivity analysis reveals complex parameter interaction patterns in dynamic models", *Chemometr. Intellig. Laborat. Syst.*, **120**, 25-41.
Vorechovsky, M. and Novak, D. (2009), "Correlation control in small-sample Monte Carlo type simulations I: A simulated annealing approach", *Prob. Eng. Mech.*, **24**, 452-462.
Wei, J.J. and Lv, Z.R. (2015), "Structural damage detection including the temperature difference based on response sensitivity analysis", *Struct. Eng. Mech.*, **53**(2), 249-260.
Ye, K.Q., Li, W. and Sudjianto, A. (2000), "Algorithmic construction of optimal symmetric Latin hypercube designs", *J. Stat. Plann. Infer.*, **90**, 145-159.
Zhao, J. and Wang, C. (2014), "Robust topology optimization under loading uncertainty based on linear elastic theory and orthogonal diagonalization of symmetric matrices", *Comput. Meth. Appl. Mech. Eng.*, **273**, 204-218.

CC

Nomenclatures

A	Cross section area of the rotor shaft
C_c	Crossover coefficient
C_e	Elitism coef ficient
C_m	Mutation coefficient
C_{eq}	Equivalent damping matrix
D^*	Diagonal matrix
d_i	Elementary effect of i_{th} input variable
E	Modulus of elasticity
F	External forces on the rotor-bearing system
G^*	Sample point matrix
G	Shear modulus
K_f	Axial force stiffness matrix
K_T	Axial torque stiffness matrix
K_{EI}	Bending stiffness matrix
K_{el}	Equivalent shaft element stiffness
K_{xx}	Bearing stiffness in direction x
K_{yy}	Bearing stiffness in direction y
$K_{\theta x \theta x}$	Bearing stiffness about axis x
$K_{\theta y \theta y}$	Bearing stiffness about axis y
l	Shaft length
M	Number of variables
M_{eq}	Equivalent inertia matrix
N	Sample size
N_m	Selected number of the closest sample point pair in mutation operation
N_c	Selected number of the closest sample point pair in crossover operation
N_p	Initial number of LHS arrays population
Q	Rotor response
$\tilde{\mathbf{Q}}$	Approximate solution of Rotor response
R_c	Number of selected genes in crossover operation
R_m	Number of selected genes in mutation operation
S_i	Sensitivity index of i_{th} input factor
ST_i	Total sensitivity index of i_{th} input factor

T	Axial torsion
T^*	Randomized orientation matrix
u	Whirling amplitude in direction x
v	Whirling amplitude in direction y
θ_x	Bending angle about axis x
θ_y	Bending angle about axis y
Δ	Step size in Morris method trajectory
μ^*	Mean parameter of the Morris method
σ	Standard deviation of the Morris method
ρ	Density
$\mathcal{K}$	Timoshenko shear coefficient
$\mathcal{R}_i$	Residual terms
$\mathcal{S}$	Shape function
ξ	Non-dimensional position coordinate

Appendix A: Rotor element shape functions

$$\begin{bmatrix} N_x \\ N_y \\ M_x \\ M_y \end{bmatrix}.\mathbf{Q} = \mathrm{S}.\mathbf{Q}$$

$$N_x = [N_1 \;\; 0 \;\; 0 \;\; -N_2 \;\; N_3 \;\; 0 \;\; 0 \;\; -N_4]$$
$$N_y = [0 \;\; N_1 \;\; N_2 \;\; 0 \;\; 0 \;\; N_3 \;\; N_4 \;\; 0]$$
$$M_x = [0 \;\; -M_1 \;\; -M_2 \;\; 0 \;\; 0 \;\; M_3 \;\; -M_4 \;\; 0]$$
$$M_y = [M_1 \;\; 0 \;\; 0 \;\; -M_2 \;\; M_3 \;\; 0 \;\; 0 \;\; -M_4]$$

$$N_1 = \frac{\left(1-3\xi^2+2\xi^3\right)+P\left(1-\xi\right)}{P+1}$$

$$N_2 = \frac{\left(\xi-2\xi^2+\xi^3\right)l+P\left(\xi-\xi^2\right)l/2}{P+1}$$

$$N_3 = \frac{\left(3\xi^2-2\xi^3\right)+P\xi}{P+1}$$

$$N_4 = \frac{\left(-\xi^2+\xi^3\right)l+P\left(-\xi+\xi^2\right)l/2}{P+1}$$

$$M_1 = \frac{\left(6\xi^2-6\xi\right)}{l\left(P+1\right)}$$

$$M_2 = \frac{\left(1-4\xi+3\xi^2\right)+P\left(1-\xi\right)}{P+1}$$

$$M_3 = \frac{\left(-6\xi^2+6\xi\right)}{l\left(P+1\right)}$$

$$M_4 = \frac{\left(3\xi^2-2\xi\right)+P\xi}{P+1}$$

$$Where := s/l, P = 12EI/(KAGl^2)$$

Appendix B: Finite element matrices

$$\boldsymbol{M}_{eq}\ddot{\tilde{\mathbf{Q}}}+\boldsymbol{C}_{eq}\dot{\tilde{\mathbf{Q}}}+\boldsymbol{K}_{eq}\tilde{\mathbf{Q}}=\boldsymbol{F}$$

$$\boldsymbol{M}_{eq}=M_{trans}+M_{rot}$$

$$M_{trans}=\frac{\rho Al}{420(P+1)^2}\begin{bmatrix} At & & & & & & & \\ 0 & At & & & & & & \\ 0 & -Dt & Bt & & & sym. & & \\ Dt & 0 & 0 & Bt & & & & \\ Et & 0 & 0 & Ft & At & & & \\ 0 & Et & -Ft & 0 & 0 & At & & \\ 0 & Ft & Ct & 0 & 0 & Dt & Bt & \\ -Ft & 0 & 0 & Ct & -Dt & 0 & 0 & Bt \end{bmatrix}$$

$$Bt=420\left(\frac{l^2}{840}+\frac{l^2}{120}(P+1)^2\right)$$

$$At=140P^2+294P+156$$

$$Ct=420\left(\frac{l^2}{840}-\frac{l^2}{120}(P+1)^2\right)$$

$$Dt=l\left(35P^2+77P+44\right)/2$$

$$Et=70P^2+126P+54$$

$$Ft=l\left(35P^2+63P+26\right)/2$$

$$M_{rot}=\frac{\rho I}{30l(P+1)^2}\begin{bmatrix} Ar & & & & & & & \\ 0 & Ar & & & & & & \\ 0 & Dr & Br & & & sym. & & \\ Dr & 0 & 0 & Br & & & & \\ -Ar & 0 & 0 & -Dr & Ar & & & \\ 0 & -Ar & Dr & 0 & 0 & Ar & & \\ 0 & -Dr & Cr & 0 & 0 & Dr & Br & \\ Dr & 0 & 0 & Cr & -Dr & 0 & 0 & Br \end{bmatrix}$$

$$Ar=36$$

$$Br=l^2\left(10P^2+5P+4\right)$$

$$Cr=-l^2\left(-5P^2+5P+1\right)$$

$$Dr=-3l\left(5P-1\right)$$

$$\boldsymbol{K}_{eq}=K_{el}+K_F+K_T$$

$$K_{el}=\frac{EI}{(P+1)l^3}\begin{bmatrix} 12 & & & & & & & \\ 0 & 12 & & & & & & \\ 0 & -6l & l^2(P+4) & & & sym. & & \\ 6l & 0 & 0 & l^2(P+4) & & & & \\ -12 & 0 & 0 & -6l & 12 & & & \\ 0 & -12 & 6l & 0 & 0 & 12 & & \\ 0 & -6l & -l^2(P-2) & 0 & 0 & 6l & l^2(P+4) & \\ 6l & 0 & 0 & -l^2(P-2) & -6l & 0 & 0 & l^2(P+4) \end{bmatrix}$$

$$K_F=\frac{F}{30l(P+1)^2}\begin{bmatrix} Af & & & & & & & \\ 0 & Af & & & & & & \\ 0 & -Cf & Bf & & & sym. & & \\ Cf & 0 & 0 & Bf & & & & \\ -Af & 0 & 0 & -Cf & Af & & & \\ 0 & -Af & Cf & 0 & 0 & Af & & \\ 0 & -Cf & Df & 0 & 0 & Cf & Bf & \\ Cf & 0 & 0 & Df & -Cf & 0 & 0 & Bf \end{bmatrix}$$

$$Af=30P^2+60P+36$$

$$Bf=l^2\left(5P^2+10P+8\right)/2$$

$$Cf=31$$

$$Df=-l^2\left(5P^2+10P+2\right)/2$$

$$K_T=\frac{T}{l(P+1)}\begin{bmatrix} 0 & & & & & & & \\ 0 & 0 & & & & & & \\ 1 & 0 & 0 & & & sym. & & \\ 0 & 1 & \frac{-l(P+1)}{2} & 0 & & & & \\ 0 & 0 & -1 & 0 & 0 & & & \\ 0 & 0 & 0 & -1 & 0 & 0 & & \\ -1 & 0 & 0 & \frac{l(P-1)}{2} & 1 & 0 & 0 & \\ 0 & -1 & \frac{-l(P-1)}{2} & 0 & 0 & 1 & \frac{l(P+1)}{2} & 0 \end{bmatrix}$$

$$\boldsymbol{C}_{eq}=Gyr$$

$$Gyr=\frac{\rho Ar^2}{60l(P+1)^2}\begin{bmatrix} 0 & & & & & & & \\ 36 & 0 & & & & & & \\ Ag & 0 & 0 & & & skew-sym & & \\ 0 & Ag & Bg & 0 & & & & \\ 0 & 36 & Ag & 0 & 0 & & & \\ -36 & 0 & 0 & Ag & 36 & 0 & & \\ Ag & 0 & 0 & Cg & -Ag & 0 & 0 & \\ 0 & Ag & -Cg & 0 & 0 & -Ag & Bg & 0 \end{bmatrix}$$

$$Ag=l\left(15P-3\right)$$

$$Bg=l^2\left(10P^2+5P+4\right)$$

$$Cg=l^2\left(-5P^2+5P+1\right)$$